

Influence of the defects of a thin NiO(100) film on the adsorption of NO

M. Bäumer, D. Cappus, G. Illing, H. Kühlenbeck, and H.-J. Freund
*Lehrstuhl für Physikalische Chemie I, Ruhr-Universität Bochum, Universitätsstrasse 150,
4630 Bochum, Germany*

(Received 26 September 1991; accepted 5 November 1991)

Defects often play an important role for the adsorption and reaction behavior of a surface. This, however, is not the case with the adsorption of NO on NiO(100), as our experiments with a thin NiO(100) film grown on a Ni(100) substrate demonstrate. This film possesses a three-dimensional band structure, which is comparable to that of a NiO(100) single crystal. A spot profile analysis low-energy electron diffraction investigation shows that the film consists of crystallites, which are tilted with respect to the Ni substrate. The film must exhibit a high defect density where the crystallites border on each other. Moreover, x-ray photoelectron spectroscopic (XPS) measurements indicate the presence of O⁻ or OH species on the surface. We have studied the adsorption of NO on a NiO(100) film via high-resolution electron energy-loss spectroscopy (HREELS), thermal desorption spectroscopy (TDS), and XPS. With HREELS and TDS we could only detect one kind of NO species on the surface. Comparing the TD and XP spectra of NO adsorbed on the film and on a bulk NiO(100) surface, which exhibits a much lower defect density, we can show that this species is NO adsorbed on regular, nondefect NiO sites.

I. INTRODUCTION

Metal oxides, especially transition metal oxides, play an essential role in the field of heterogeneous catalysis as catalysts and as supports.^{1,2} Therefore the study of their adsorption and reaction behavior is of great importance. The fact that surface science has only recently turned towards this field is mainly due to experimental difficulties: because of the limited conductivity of these compounds electron spectroscopic techniques result in charging of the samples, which can seriously complicate the interpretation. This problem may be circumvented by using thin films, which can be epitaxially grown on metal surfaces, instead of oxide bulk materials.

Concerning NiO it is already known from literature that a thin NiO(100) film grows on a Ni(100) surface under appropriate preparation conditions.³ But in contrast to a bulk NiO(100) surface cleaved in vacuo, this film has very broad and diffuse low-energy electron diffraction (LEED) spots,⁴⁻⁶ which are probably an indication of a rather disturbed surface structure.

The aim of our investigation was to describe the geometric and electronic structure of such a film in detail and to study the adsorption of NO on this oxide layer. We have characterized the structure with the help of profile analysis of the LEED spots [spot profile analysis low-energy electron diffraction (SPA-LEED)]. For additional information about the nature of the defects existing on the surface x-ray photoelectron spectroscopic measurements (XPS) have been carried out. By using angle resolved ultraviolet photoelectron spectroscopy (ARUPS), we have mapped the electronic band structure of the film and compared it to the band structure of the bulk system. After having characterized the properties of the clean film, we have studied the NO adsorption via high-resolution electron energy-loss

spectroscopy (HREELS), thermal desorption spectroscopy (TDS), and XPS. The results have been compared to data which have been taken on an in vacuo cleaved NiO(100) single crystal.

II. EXPERIMENT

We have performed the experiments in different ultrahigh vacuum (UHV) systems. The ARUP spectra have been taken at the storage ring BESSY (Berliner Elektronenspeicherringesellschaft für Synchrotronstrahlung mbH). A SPA-LEED system⁷ of the type Leybold SPA-LEED 11 with a specified transfer width of 900 Å was used for the analysis of the LEED spot profiles. XP spectra of the NiO(100) film have been recorded in a spectrometer equipped with a monochromatized Al-K_α source (Leybold AG). The HREELS data have been taken in a UHV system equipped with a Leybold ELS22 system with a typical resolution of 8 meV. The cleanliness of the Ni(100) samples was always checked with the help of Auger electron spectroscopy (AES).

The details of the instrumentation used for the experiments with the bulk NiO(100) sample have been described elsewhere.⁶

The Ni crystals were spot welded to two tungsten rods, which were connected to a liquid nitrogen reservoir such that the sample could be cooled below 100 K. Heating was possible by radiation from a filament mounted behind the crystal or by electron bombardment onto the reverse side of the crystal. The surface was prepared by repeated cycles of sputtering with Ne ions and heating to 800 K. Residual carbon was then removed by flashing the crystal in an oxygen atmosphere of 10⁻⁷ mbar followed by heating the crystal to 700 K for several minutes in 10⁻⁷ mbar hydro-

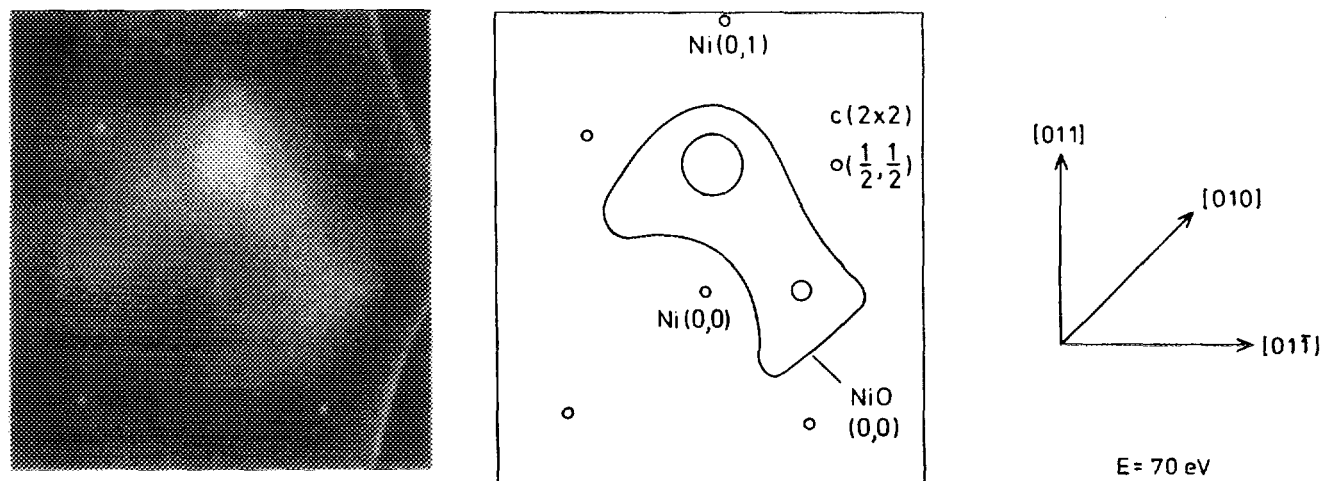


FIG. 1. LEED pattern of the thin NiO(100) film taken with the SPA-LEED instrument. The sharp spots belong to the Ni(100) substrate and a $c(2 \times 2)$ superstructure of chemisorbed oxygen. The formation of the $c(2 \times 2)$ structure always precedes the growth of the oxide film.

gen until LEED and AES indicated a clean and well-ordered surface.

The NiO(100) film was prepared by repeated cycles of dosing 1200 L O_2 (1 L = 10^{-6} Torr s) at $p(O_2) = 10^{-5}$ Torr and $T = 570$ K and subsequent annealing to $T = 660$ K up to an oxygen exposure of about 10 000 L. After this treatment the LEED pattern exhibited broad NiO(100) spots. The Ni(100) substrate spots were strongly attenuated and additionally weak $c(2 \times 2)$ reflexes of an oxygen superstructure were visible.

III. RESULTS AND DISCUSSION

A. The structure of the NiO(100) film

1. SPA-LEED data

The Ni(100) crystal used for the SPA-LEED investigation exhibits a regular monotonic step array as a result of a 1° misorientation of the surface. This was determined via profile analysis of the (0,0) LEED reflex: As it is typical of such a step array, the spot showed a periodic splitting in the [010] direction as a function of the electron energy.^{8,9} The step height, as deduced from the energy dependence, amounts to 1.76 Å (monoatomic steps). The terrace length, which can be determined from the distance of the splitted spots in K space, is of the order of 100 Å.

The preparation of the NiO(100) film was carried out as described in Sec. II. After an oxygen exposure of 10 000 L the crystal showed the LEED pattern depicted in Fig. 1. This figure reveals that the NiO-(0,0) and the Ni-(0,0) reflex are not found at the same position as often described in the literature.^{4,5} Instead, the NiO-(0,0) reflex is semi-circularly distributed around the substrate spot with two distinct maxima in the [011] and [01 $\bar{1}$] direction. A similar situation exists for reflexes of higher order. The relative intensities of the two maxima vary as a function of the position of the beam on the crystal.

We have determined the distances between the maxima and the Ni-(0,0) reflex and their full widths at half-maximum (FWHM) as a function of the electron energy.

Unfortunately, there were only some energy ranges where the NiO spots exhibited sufficient count rates. The data are listed in Table I: obviously, the values for both quantities increase monotonously with energy. This behavior is characteristic of a mosaic structure,⁹⁻¹¹ i.e., the film consists of crystallites, which are tilted with respect to the Ni(100) surface normal.

We have characterized the distribution of the tilting angles by two parameters: the most frequent tilting angle α of the crystallites, which can be calculated from the shifts of the profile maxima, and the halfwidth of the tilting angle distribution $\delta\alpha$, which is obtainable from the halfwidths of the profiles. The results of this quantitative evaluation of the experimental data are also given in Table I. Except for small statistical deviations, the values do not vary with beam energy as expected for the proposed structure model. The average values for α and $\delta\alpha$ amount to $\alpha = 8.0^\circ$ and $\delta\alpha = 6.7^\circ$.

The crystallites are tilted along those directions in which intensity of the NiO-(0,0) reflex is shifted. But the

TABLE I. Distances between the the Ni-(0,0) reflex and the maxima of some NiO reflexes and the profile halfwidths. The values are given in percent of the [011] reciprocal lattice vector of the Ni(100) surface Brillouin zone. For $E = 200$ eV the Ni-(0,0) spot was not visible and so the corresponding distance is missing in the fourth column.

E (eV)	Reflex	Direction of scan	Distance (% BZ)	FWHM		
				[% Brillouin zone (BZ)]	α (deg)	$\delta\alpha$ (deg)
65	(0,0)	[011]	46.2	38.2	8.1	6.7
70	(0,0)	[011]	49.5	40.3	8.4	6.8
75	(0,0)	[011]	49.5	38.2	8.1	6.3
110	(0,0)	[011]	57.0	47.5	7.7	6.4
120	(0,0)	[011]	60.9	52.6	7.9	6.8
130	(0,0)	[011]	63.7	54.7	7.9	6.8
200	(0,0)	[011]	...	65.0	...	6.5
45	(1,0)	[01 $\bar{1}$]	117.5	28.5	7.5	6.6
50	(1,0)	[01 $\bar{1}$]	123.2	29.4	8.2	6.5
85	(2,0)	[01 $\bar{1}$]	215.7	38.0	8.3	7.1

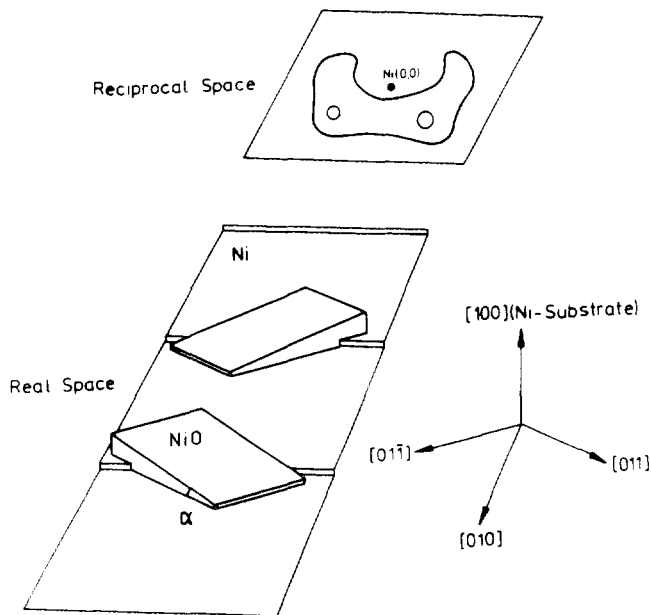


FIG. 2. Schematic plot showing the steps of the Ni substrate and two NiO crystallites tilted along the main tilting directions.

occurrence of the intensity maxima clearly reveals that the $[011]$ and $[0\bar{1}1]$ direction are preferred. If we remember that the descending step direction on the Ni substrate was $[010]$, it is realized that a correlation exists between the tilting direction and the step direction. In order to illustrate this, a schematic plot is presented in Fig. 2, which shows two NiO crystallites tilted in the $[011]$ and $[0\bar{1}1]$ direction and the steps on the Ni substrate. The figure allows two conclusions:

(a) there are no crystallites tilted in an ascending step direction of the substrate;

(b) a preferred tilting is observed along those $[011]$ -like directions which are near the descending step direction on the substrate. These results are in line with a scanning tunneling microscopic (STM) study of the film, which has been performed by Neddermeyer and co-workers.¹²

The question near at hand is how the formation of the mosaic structure can be explained. We are convinced that the starting point for an answer is the large mismatch of the lattice constants of Ni and NiO [$a(\text{NiO}) = 4.16 \text{ \AA}$, $a(\text{Ni}) = 3.52 \text{ \AA}$ (Ref. 13)]. Due to this mismatch, considerable lattice stress must occur during the growth of the film, which may be reduced by a tilting of small oxide crystallites. Probably, the Ni atoms at the step edges of the Ni surface support this process by migrating underneath the crystallites and lifting them. However, we found no explanation concerning the observed preference for $[011]$ -like tilting directions on the basis of our results.

It should be mentioned that the adsorption experiments described in Sec. III C were carried out with different Ni substrates. The NiO films which were not grown on the Ni crystal used for the SPA-LEED investigation did not always show LEED patterns with shifted NiO spots. After all preparations, however, we obtained broad reflexes indicating that the film growth always led to the formation of

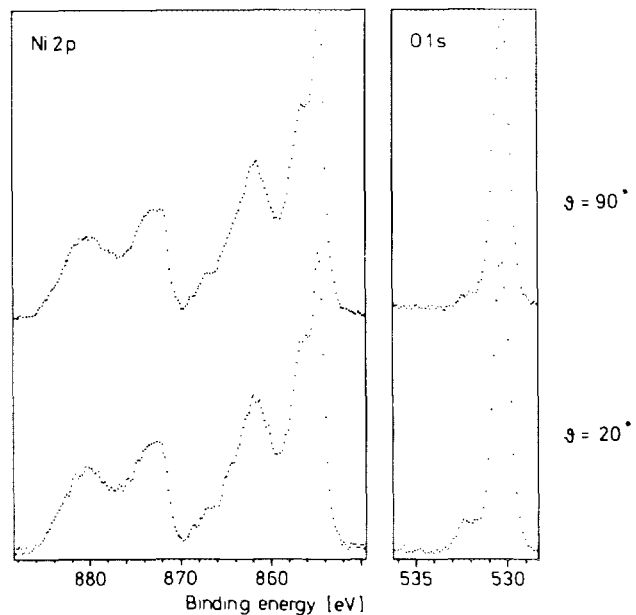


FIG. 3. Ni 2p and O 1s XP spectra for the NiO(100) film taken at different collection angles θ .

a mosaic structure with a wide spread of tilting angles. As discussed above, a shift of the NiO reflexes is due to a most frequent tilting angle α greater than 0° . Consequently, a LEED pattern with unshifted reflexes reveals that this quantity equals zero. We suppose that this situation is encountered for NiO films which are grown on Ni surfaces with no misorientation.

2. XPS data

The Ni 2p and O 1s spectra of the studied NiO(100) film are shown in Fig. 3. Data with varying surface sensitivity (by changing the electron collection angle) for both, the Ni 2p and O 1s bands, are included in the figure. At normal emission, i.e., at lowest surface sensitivity, the O 1s signal appears to be rather symmetric, although there is already a slight indication of a feature at 532.3 eV binding energy, which can be clearly recognized in the spectrum with higher surface sensitivity. It is independent of the preparation conditions and cannot be removed by heat treatment without destroying the NiO(100) film itself.

However, the Ni 2p signal does not show any significant dependence on the collection angle in line with results on a NiO(100) single crystal¹⁴ (see however Ref. 15). Therefore it is possible to connect the feature at 532.3 eV with defects in the oxygen sublattice at the surface. Water adsorption, which leads to signals in the same range of binding energies, can be excluded due to a low thermal stability.¹⁶ Consequently, we suspect that the peak is indeed correlated with oxygen defect states. Possibilities would be O^- and OH.

B. The electronic structure of the NiO(100) film

The upper graph in Fig. 4 shows the valence-band structure of the NiO(100) film in the Δ direction, which we

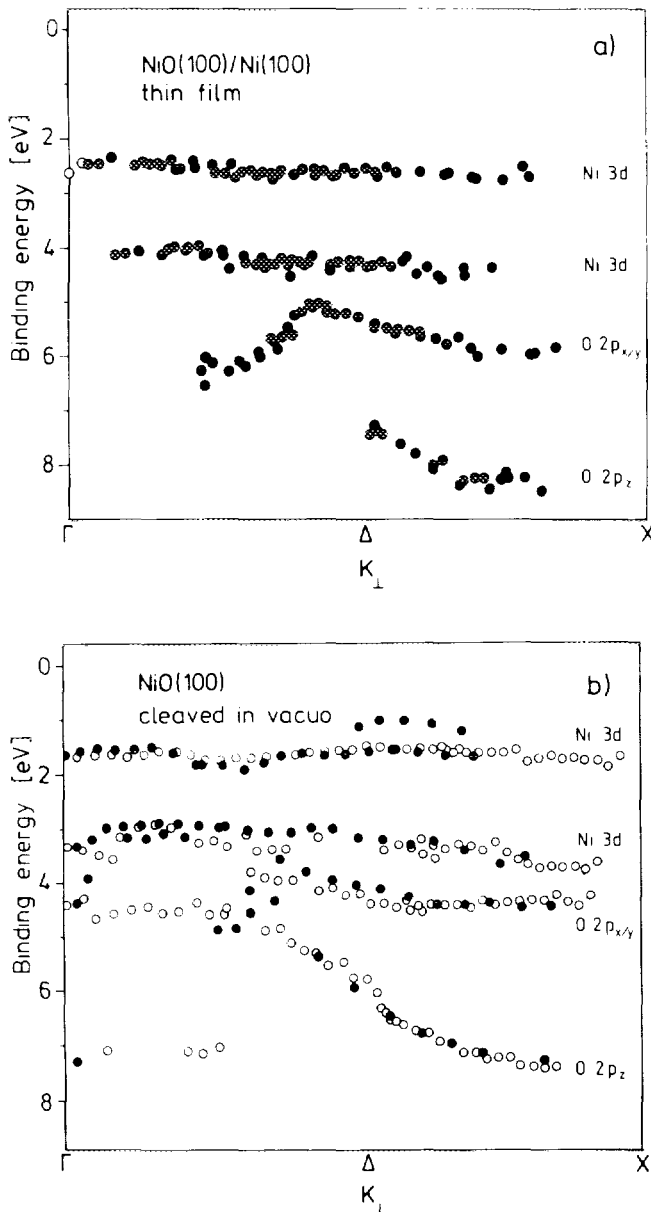


FIG. 4. Valence-band structures for NiO(100)/Ni(100) [panel (a)] and in vacuo cleaved NiO(100) [panel (b)] perpendicular to the surface. Solid circles represent data points in the first half of the second Brillouin zone, whereas open circles are data points folded back from the second half of the second Brillouin zone.

have obtained from ultraviolet photoelectron (UP) spectra taken at normal emission with different photon energies.⁶ For comparison Fig. 4 also contains the corresponding band structure of a NiO(100) single crystal cleaved in vacuo, which was determined by M. Neumann and co-workers.⁶ The inspection of the two sets of dispersion curves allows the conclusion that the electronic structure of both systems is very similar perpendicular to the surface. This means that the film is thick enough to develop a three-dimensional band structure.

Apart from the Δ direction we have also probed the dispersion of the four electronic states along directions parallel to the surface and found a far-reaching correspondence between the curves of the film and the bulk material

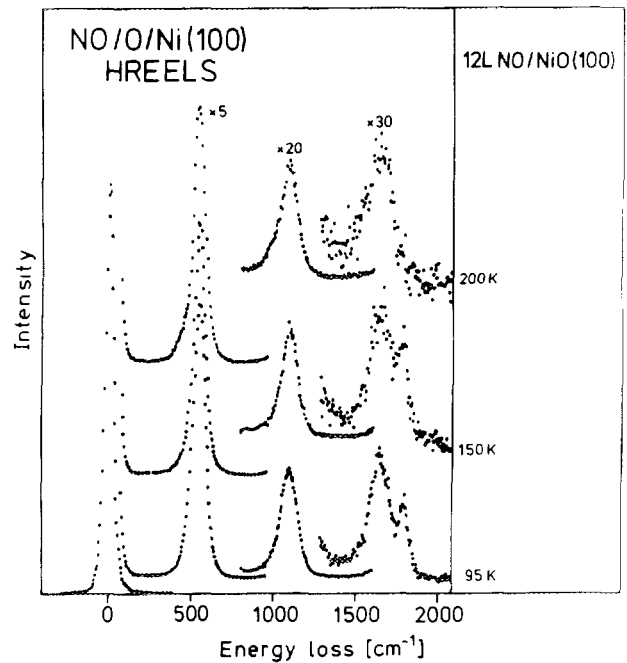


FIG. 5. HREEL spectra of NO adsorbed on the NiO(100) film at three different temperatures.

again. Hence, the analysis of the electronic structure of the film reveals that it exhibits characteristics comparable to that of bulk NiO.

C. Adsorption of NO

We have investigated the adsorption of NO on the NiO(100) film employing HREELS, TDS, and XPS.⁶

In Fig. 5 the HREEL spectrum taken after 12 L NO exposure at 95 K as well as the spectra recorded after heating the sample to 150 and 200 K are shown. We always find intense features at 560, 1120, and 1680 cm⁻¹, which originate from the excitation of Fuchs-Kliewer-phonons on the surface.⁵ The adsorbed NO leads to one additional peak at 1800 cm⁻¹, which we assign to a NO stretching mode. It disappears after heating the sample to 200 K. Within the experimental resolution of the spectrometer, the spectra indicate that there is one single NO adsorption site on the NiO(100) film, with a desorption temperature of 200 K.

Considering the defects which should exist in the regions between the flat crystallite surfaces, it would be expected that NO adsorbs onto one of these defect sites. However, that is not the case as shown in Fig. 6, where TDS traces of NO adsorbed on the NiO(100) film and on an almost defect-free bulk NiO(100) surface are compared. Due to the close correspondence of the two spectra, we conclude that NO adsorbs on regular NiO sites with an adsorption energy of 0.52 eV as deduced from application of the Readhead equation. The value indicates that NO is weakly chemisorbed on NiO(100).

Our XP spectra, shown in Fig. 7, corroborate the interpretation based on the TDS results. Again, because of the close correspondence of the N 1s spectra recorded for NO

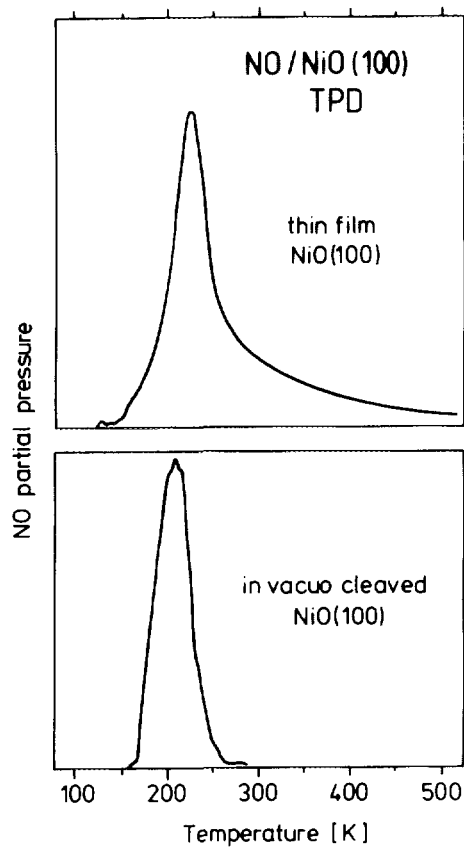


FIG. 6. Comparison of thermal desorption spectra for NO adsorbed on the NiO(100) film and on a cleaved NiO(100) single crystal sample.

on the film and on the bulk surface, we must deduce that NO adsorbs on nondefect NiO sites. The existence of two peaks in the N 1s spectra is not connected with two NO species on the surface but rather with so-called "giant" shake-up intensities. As discussed elsewhere,⁶ the two peaks are due to screening of the core hole created in the photoionization process and are assigned to the screened (low binding energy) and unscreened state (high binding energy) of the molecular N 1s hole state. The NO O 1s

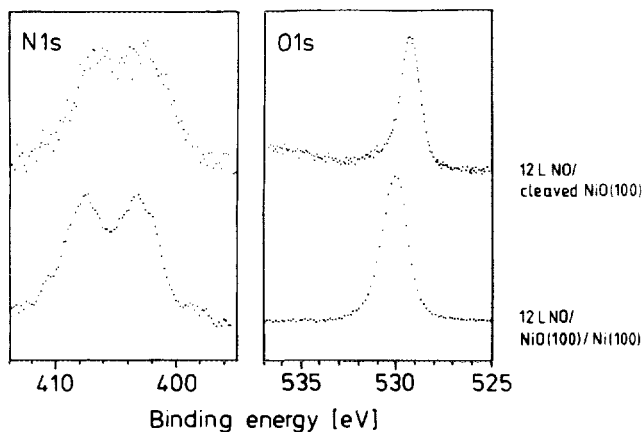


FIG. 7. Set of N 1s and O 1s XP spectra for NO adsorbed on the film and the cleaved NiO surface.

emission is not recognized in the data due to interference with the oxide O 1s signals.

IV. SUMMARY AND CONCLUSIONS

(1) On a Ni(100) substrate a NiO(100) film can be grown which is thin enough to prevent charging of the surface when electron spectroscopic techniques are applied.

(2) This film consists of small crystallites, which are tilted with respect to the Ni surface normal. The tilting is correlated with steps on the substrate surface.

(3) The film exhibits a three-dimensional electronic band structure, which is comparable to that of a NiO single crystal.

(4) A large amount of different kinds of defects must exist on the film where the crystallites border on each other. Contrary to expectations, NO does not adsorb on these defect sites, i.e., the regular NiO sites are preferred.

ACKNOWLEDGMENTS

This work has been supported by the German Federal Minister for Research and Technology (B.M.F.T.), the Minister for Science and Research of the State Nordrhein-Westfalen (M.W.F.), and the Deutsche Forschungsgemeinschaft. H.-J. F. thanks the Fonds der chemischen Industrie for financial support.

¹V. F. Kiselev, O. V. Krylov, *Adsorption and Catalysis on Transition Metals and Their Oxides*, Springer Series in Surface Sciences Vol. 9 (Springer, Berlin, 1989).

²A. B. Stiles, *Catalyst Supports and Supported Catalysts* (Butterworths, Boston, 1987).

³W.-D. Wang, N. J. Wu, and P. A. Thiel, *J. Chem. Phys.* **92**, 2025 (1990).

⁴P. H. Holloway and J. B. Hudson, *Surf. Sci.* **43**, 123 (1974).

⁵G. Dalmai-Imelik, J. C. Bertolini, and J. Rousseau, *Surf. Sci.* **63**, 67 (1977).

⁶H. Kuhlenbeck, G. Odörfer, R. Jaeger, G. Illing, M. Menges, T. Mull, H.-J. Freund, M. Pöhlchen, V. Staemmler, S. Witzel, C. Scharf-schwerdt, K. Wennemann, T. Liedke, and M. Neumann, *Phys. Rev. B* **43**, 1969 (1991).

⁷U. Scheithauer, G. Meyer, and M. Henzler, *Surf. Sci.* **178**, 441 (1986).

⁸M. Henzler, in *Electron Spectroscopy for Surface Analysis*, Topics in Current Physics Vol. 4, edited by H. Ibach (Springer, Berlin, 1977).

⁹M. G. Lagally, in *Solid State Physics: Surfaces*, Methods of Experimental Physics Vol. 22, edited by R. L. Park and M. G. Lagally (Academic, New York, 1985).

¹⁰D. G. Welkie and M. G. Lagally, *J. Vac. Sci. Technol.* **17**, 453 (1980).

¹¹H. M. Clearfield, D. G. Welkie, T. M. Lu, and M. G. Lagally, *J. Vac. Sci. Technol.* **19**, 323 (1981).

¹²M. Bäumer, D. Cappus, H. Kuhlenbeck, H.-J. Freund, G. Wilhelm, A. Brodde, and H. Neddermeyer, *Surf. Sci.* **253**, 116 (1991).

¹³Landolt-Börnstein, *Zahlenwerte aus Physik, Chemie, Astrophysik, Geophysik und Technik* (Springer, Berlin, 1955), Vol. 1, Part 4.

¹⁴M. Oku, H. Tokuda, and K. Hirokawa, *J. Electron Spectrosc. Relat. Phenom.* **53**, 201 (1991).

¹⁵F. Parmigiani, P. S. Bagus, and G. Pacchioni (submitted).

¹⁶G. Illing, Ph. D. thesis, Universität Bochum, Germany, 1991.